Dynamical Coarse-Graining of Highly Fluctuating Membranes under Shear Flow

Simon W. Marlow* and Peter D. Olmsted†
Polymer IRC and Department of Physics & Astronomy, University of Leeds, Leeds LS2 9JT, United Kingdom

(Dated: February 1, 2008)

The effect of strong shear flow on highly fluctuating lamellar systems stabilized by intermembrane collisions via the Helfrich interaction is studied. Advection enters the microscopic equation of motion for a single membrane via a non-linear coupling. Upon coarse-graining the theory for a single bilayer up to the length scale of the collision length, at which a hydrodynamic description applies, an additional dynamical coupling is generated which is of the form of a wavevector-dependent tension that is non-linear in the applied shear rate. This new term has consequences for the effects of strong flow on the stability and dynamics of lamellar surfactant phases.

PACS numbers: 61.30.Dk Continuum models and theories of liquid crystal structure, 05.10.Cc Renormalization group methods, 87.16.Dg Membranes, bilayers, and vesicles

I. INTRODUCTION AND OVERVIEW

Dilute solutions of lamellar phases typically consist of highly fluctuating layers. The wide equilibrium layer spacings are governed by the interplay between the long-range steric repulsion, known as the Helfrich interaction [1], and the bending elasticity of the bilayers. When these systems undergo flow, a range of interesting phenomena is observed, transitions to multilamellar vesicles [2, 3] and a reduction in layer spacing [4]. Unlike layered one component melts, such as thermotropic smectics or diblock copolymers, flow can have a significant effect on the microstructure of the layers. Although flow certainly stretches the chains in diblock copolymers [5] and can induce layer tilt in thermotropic smectics [6], the effect on the highly-fluctuating many-component layered surfactant phases should be much more dramatic.

As an initial step to account for some of this flow behaviour, we previously conjectured [7] that flow induces an effective anisotropic tension parallel to the flow, when lamellae are aligned in the c orientation (Fig. 1). The "tension" is a response to projected area changes and acts to suppress the fluctuations. This led to predictions for either changes in layer spacing or an undulation instability. In a related work, Zilman and Granek [8] also proposed an effective tension, but isotropic, negative in sign, and of a different physical origin. While both studies relied on inserting the "tension" heuristically into the dynamics as an effective free energy term, it is of interest to examine the dynamics of a membrane in flow to see how such a response can be generated dynamically. In this work we consider a lamellar phase stabilized by the Helfrich interaction, neglecting the effect of electrostatic forces. By coarse-graining the dynamics up to a length scale characteristic of the long wavelength hydrodynamic description, the typical transverse length L_p between collisions, we demonstrate that flow can indeed induce a dynamical suppression of fluctuations that resembles a wavevector-dependent "tension".

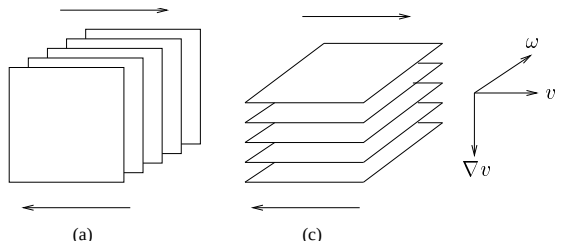

FIG. 1: The allowable steady state orientations a and c of a lamellar phase in uniform shear flow.

The linearized relaxational dynamics of a membrane parametrized by a single height variable h subject to an anisotropic tension σ, written in Fourier space, is

$$\partial_t h(\boldsymbol{q}) = -\Lambda(\boldsymbol{q}) \left[\kappa q^4 + \sigma q_x^2\right] h(\boldsymbol{q}), \qquad (1.1)$$

where κ is the bending modulus, $\boldsymbol{q}$ is the wave vector and the kinetic coefficient $\Lambda(\boldsymbol{q})$ depends on the particular relaxation mechanism. The tension penalizes fluctuations and, if applied to a stack of such membranes that interact via collisions, would change the "preferred" layer spacing and renormalize the coarse-grained smectic layer compression modulus $\bar{B}$. Our task here is to derive an equivalent term that would contribute to the effective dynamics of highly fluctuating membranes in shear flow in the c orientation, $\boldsymbol{v} = \dot{\gamma} z \hat{\boldsymbol{x}}$. We shall find that the equation of motion for the coarse-grained height field in shear flow becomes

*Electronic address: physwm@irc.leeds.ac.uk
†Electronic address: p.d.olmsted@leeds.ac.uk

$$\partial_t h(\boldsymbol{q}) + i\dot{\gamma}\sum_{\boldsymbol{k}}(q_x - k_x)h(\boldsymbol{k})h(\boldsymbol{q}-\boldsymbol{k}) = -\left\{\Lambda(\boldsymbol{q})\kappa q^4 + \Lambda_x q_x^2\right\}h(\boldsymbol{q}), \qquad \left(q > \frac{\pi}{L_p}\right) \tag{1.2}$$

where the function Λ_x depends on the wave vector, the strain rate $\dot{\gamma}$, the kinetic coefficient $\Lambda(\boldsymbol{q})$, and the coarse-graining length. The non-linear advection term, which arises from assuming an affine distortion of the membrane, induces the non-trivial renormalization of the dynamics under coarse-graining. Hence, the "tension", as such, is given by

$$\sigma = \Lambda_x \Lambda^{-1}(\boldsymbol{q}) \tag{1.3}$$

and is a function of the strain rate and is typically wave vector dependent.

Our calculation is similar to renormalization group calculations of the anisotropic Burgers equation, studied in the context of sandpiles [9], and of phase separating systems under shear flow [10, 11]. However, unlike the calculation of critical behavior, in which coarse-graining proceeds until scaling is found, coarse-graining in our case can only be performed up to the natural physical cutoff corresponding to the collision length L_p. This may or may not be in the scaling regime; if it is not, then there are generally other terms generated by the coarse-graining procedure. However, such a calculation is generally impossible, so instead we estimate the coarse-grained dynamics from that obtained by a non-trivial scaling fixed point calculation. Moreover, we expect that terms that eventually become irrelevant in the scaling regime are in the process of being driven close to zero at the true coarse-graining length L_p, and in any case are of higher wave vector and hence not present in a hydrodynamic description.

Our one loop perturbation expansion of the dynamics yields, for any $\Lambda(\boldsymbol{q})$, a tension that scales as $\sigma \sim \dot{\gamma}^2$. By considering the energetic cost involved in bending and stretching a single membrane, Zilman and Granek [8] estimated a tension (isotropic) with the same scaling. However, upon performing a coarse-graining one finds a dependence $\sigma \sim \dot{\gamma}^{\varepsilon}$, where ε depends on $\Lambda(\boldsymbol{q})$.

In Section II we summarize single membrane relaxation dynamics, discuss previous studies of the dynamics of h and the coarse-grained smectic displacement variable u in shear flow and derive the equation of motion for a membrane in shear in the c orientation. In Section III we outline the coarse-graining procedure and extract results for the renormalized dynamics, for different relaxation mechanisms. We conclude in Section IV with a discussion. The appendices collect calculations of the permeation dynamics and the details of the renormalization calculation.

II. MEMBRANE DYNAMICS

A. Membrane Dynamics without Shear Flow

First we review the equilibrium properties of a Helfrich-stabilized lamellar phase, in preparation for studying its dynamics in flow. The long-ranged entropic interaction, characteristic of such a phase, is a consequence of colliding membranes due to thermal fluctuations. A key notion is the characteristic distance L_p between the collisions, marking the transition in length scale between the membrane and bulk smectic behaviour. This enables us to relate the static behaviour of a single membrane at a mean layer spacing ℓ to the compression elasticity of the lamellar phase.

In general, if $h(\boldsymbol{x}, t)$ is the height of a membrane above a plane in d dimensional space, where $\boldsymbol{x} = (x, \boldsymbol{x}_\perp)$ is a $(d-1)$ dimensional vector in the plane and t is time, the elastic free energy in the Monge gauge ($\langle(\boldsymbol{\nabla}h)^2\rangle \ll 1$) is given by the Helfrich Hamiltonian [1],

$$\mathcal{H} = \tfrac{1}{2}\kappa \int d^{d-1}x \left(\nabla^2 h(\boldsymbol{x})\right)^2 \tag{2.1}$$

where the bending modulus κ has dimensions of (energy)$*$(length)$^{3-d}$. For the rest of the paper we use discrete or continuous Fourier transforms as convenient,

$$h(\boldsymbol{x},t)=\begin{cases}\displaystyle\sum_{\boldsymbol{q}}\sum_{\omega}h(\boldsymbol{q},\omega)e^{i(\boldsymbol{q}\cdot\boldsymbol{x}-\omega t)} & \text{(discrete)}\\ \displaystyle\int_{-\infty}^{+\infty}\frac{d\omega}{2\pi}\int_{\boldsymbol{q}}\frac{d^{d-1}\boldsymbol{q}}{(2\pi)^{d-1}}h(\boldsymbol{q},\omega)e^{i(\boldsymbol{q}\cdot\boldsymbol{x}-\omega t)} & \text{(continous),}\end{cases} \tag{2.2}$$

where $\boldsymbol{q}=q_x\hat{x}+\boldsymbol{q}_\perp\cdot\hat{\boldsymbol{x}}_\perp$ and ω is the frequency. For clarity we reproduce results in the rest of this section for $d=3$ so that $\boldsymbol{x}_\perp=y\hat{\boldsymbol{y}}$. In terms of the Fourier components $h(\boldsymbol{q})$, the equipartition theorem gives the equilibrium height correlation function $\langle|h(\boldsymbol{q})|^2\rangle=T/\kappa|\boldsymbol{q}|^4$, where we take the Boltzmann constant $k_B=1$. The statistics of small fluctuations with wave vectors $qL_p>1$ are adequately determined by the Helfrich Hamiltonian. However, the behaviour of large fluctuations with wave vectors $qL_p<1$, is complicated by the steric repulsion. Constraining the fluctuations to within a layer spacing determines the mean transverse length L_p between collisions, which scales as $L_p\sim\ell\sqrt{\kappa/T}$. The loss of entropy associated with each collision contributes to the free energy change of the lamellar stack under a change of layer spacing, and hence a bulk compression modulus that scales as $B\sim T^2/\kappa\ell^3$ [1]. Long wavelength ($qL_P<1$) lamellar behaviour is described in terms of the displacement u of the mean layer position from its mean value, defined by

$$u(x,y,z=n\ell)=\int_{A(L_p)}\left[h(x'-x,y'-y)-n\ell\right]\frac{d^2x'}{A(L_p)}, \tag{2.3}$$

where $A(L_p)$ is the typical membrane area per collision. Bulk equilibrium smectic behavior can be obtained by removing the small wavelength, high q, height degrees of freedom h, until a coarse-grained description entirely in terms of the long wavelength variable u remains [12]. Our goal is to carry out this procedure for the dynamics of a single fluctuating membrane in flow, by coarse-graining the dynamical description up to the collision length. A complete calculation would naturally need to simultaneously incorporate the steric repulsion.

The relaxation dynamics of a single membrane can be described by a Langevin equation,

$$\partial_t h(\boldsymbol{x},t)=-\int d^2x'\Lambda\left(\boldsymbol{x}-\boldsymbol{x}'\right)\frac{\delta\mathcal{H}}{\delta h(\boldsymbol{x}',t)}+\xi(\boldsymbol{x},t), \tag{2.4}$$

where the thermal noise $\xi(\boldsymbol{q},t)$ describes the neglected microscopic degrees of freedom. The noise has zero mean and a variance given by the Fluctuation Dissipation Theorem,

$$\langle\xi(\boldsymbol{q}_1,t_1)\xi(\boldsymbol{q}_2,t_2)\rangle=2T\Lambda(\boldsymbol{q}_1)\delta\left(\boldsymbol{q}_1+\boldsymbol{q}_2\right)\delta\left(t_1-t_2\right). \tag{2.5}$$

A spatial Fourier transformation gives

$$\partial_t h(\boldsymbol{q},t)=-\Lambda(\boldsymbol{q})\frac{\delta\mathcal{H}}{\delta h(-\boldsymbol{q})}+\xi(\boldsymbol{q},t). \tag{2.6}$$

The kinetic function $\Lambda\left(\boldsymbol{q}\right)$ depends on the details of the fluid-membrane coupling; a general form is

$$\begin{aligned}\Lambda(\boldsymbol{q})&=\Lambda_0|\boldsymbol{q}|^m\\&\sim\eta^{-1}l^{m+1}|\boldsymbol{q}|^m,\end{aligned} \tag{2.7}$$

where the exponent m and the associated length scale l depend on the relaxation mechanism.

Three relaxation mechanisms are summarized in Fig. 2 with relaxation functions given by

$$\Lambda(\boldsymbol{q})\sim\begin{cases}\eta^{-1}q^{-1} & m=-1, \quad \text{isolated}\\ \eta^{-1}\zeta q^0 & m=0, \quad \text{permeable}\\ \eta^{-1}\ell^3q^2 & m=2, \quad \text{confined fluid.}\end{cases} \tag{2.8}$$

Thin, impermeable membranes exhibit two regimes: (i) ($m=-1$) For $q^{-1}>\ell$ the membrane is damped by viscous solvent drag. Solving the linearized Navier-Stokes equations for the solvent flow yields $\Lambda(\boldsymbol{q})=1/4\eta q$ [13], whence $i\omega=\kappa q^3/4\eta$. (ii) ($m=2$) For $q^{-1}<\ell$, solvent flow is screened by the surrounding membranes, leading to $i\omega=\kappa\ell^3q^6/16\eta$ [14]. Permeable membranes exhibit an additional regime. (iii) ($m=0$) For $\zeta<q^{-1}<\ell$ where ζ is a permeation length scale that depends on the size and the density of microscopic defects and membrane thickness, $\Lambda(\boldsymbol{q})\sim\zeta/\eta$. A simple model of cylindrical pores (common in lamellar phases) of width w and mean separation R leads to $\zeta\sim R^2\tau/w^4$, where τ is the thickness of the membrane (see Appendix A). We may envisage particular systems in which, at sufficiently high permeabilities $\zeta^{-1}<\ell^{-1}$ the isolated regime is excluded, and others for which $\zeta^{-1}<L_p^{-1}$ so that only the permeable regime remains.

B. Equations of Motion in Shear Flow

1. *Previous studies: linear advection*

Before we consider the dynamics of a single fluctuating membrane in flow in the c orientation, we review the equations of motion previously used to describe lamel-

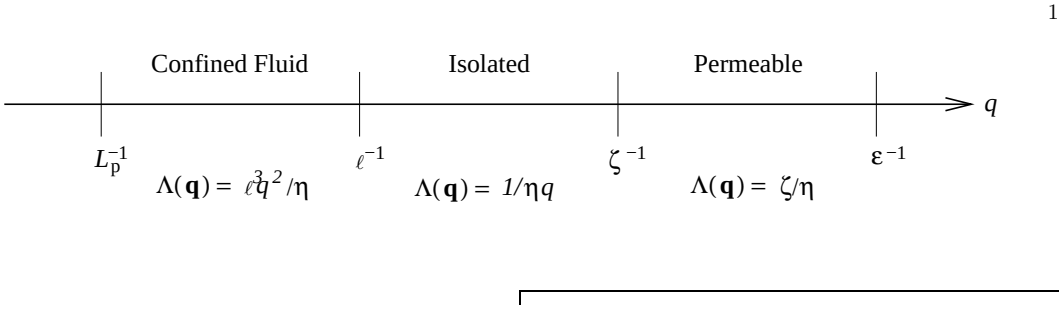

FIG. 2: Different scaling regimes for the kinetic coefficient. ζ is the permeation length and ε is the length at which the dynamical description breaks down.

lar phases in flow. Milner and Goulian [15] explored the stability with respect to a and c orientations of a thermotropic smectic under flow. Since the layer fluctuations of most thermotropic systems are small relative to the length scale of the layer spacing, shear will not have a significant effect on the shape of the layers or the internal structure. Thus the appropriate parametrization is entirely in terms of the broken symmetry smectic displacement variable $u(\mathbf{r})$. In flow, this quantity simply advects as a passive scalar. In simple shear flow with average flow velocity parallel to $\hat{\boldsymbol{x}}$, and velocity gradient direction $\hat{\boldsymbol{n}}$, the flow field is

$$\begin{aligned} \boldsymbol{v}(\boldsymbol{r}) &= (\boldsymbol{r}\cdot\hat{\boldsymbol{n}})\dot{\gamma}\hat{\boldsymbol{x}} \\ \hat{\boldsymbol{n}} &= \cos\theta\hat{\boldsymbol{z}} + \sin\theta\hat{\boldsymbol{y}}. \end{aligned} \tag{2.9}$$

where $\hat{\boldsymbol{n}} = \hat{\boldsymbol{y}}$ in the a orientation and $\hat{\boldsymbol{n}} = \hat{\boldsymbol{z}}$ in the c orientation. In this case, the dynamics of the smectic phase is

$$\left(\partial_t - \dot{\gamma} q_x \hat{\boldsymbol{n}}\cdot\frac{\partial}{\partial \boldsymbol{q}}\right) u(q,t) = -\beta(q)\frac{\delta\mathcal{F}}{\delta u(q,t)} + \chi(\boldsymbol{q},t) \tag{2.10}$$

where $\mathcal{F}$ is the smectic free energy, $\chi(\boldsymbol{x},t)$ is the noise and $\beta(q)$ is the smectic kinetic coefficient. After minimising an effective free energy expanded in powers of strain rate, Milner and Goulian showed that the a orientation is stable with respect to the c orientation; moreover, they demonstrated that a more rigorous calculation of the dynamic response function incorporating non-linear terms in the free energy exhibits the same result.

Earlier, Bruinsma and Rabin [16] studied the effect of shear on a lyotropic smectic phase in the c orientation. In most of their calculations they assumed that flow doesn't change the membrane shape and character, and hence considered the same passive advection of u when calculating the effect of shear on the smectic hydrodynamic dispersion relations. However, they did consider the degree to which flow influences the microscopic height variable h, and estimated the shear rate $\dot{\gamma}_c$ at which an affine deformation of individual membranes leads to significant suppression of fluctuations,

$$\dot{\gamma}_c = \frac{T^{5/2}}{\kappa^{3/2}\eta\ell^3}. \tag{2.11}$$

This was obtained using, effectively, the isolated impermeable membrane approximation ($m = 0$) for $\Lambda(\boldsymbol{q})$.

Finally, Ramaswamy predicted that a dilute Helfrich-stabilized lamellar phase collapses when subjected to a flow field $\boldsymbol{v} = \dot{\gamma} y\hat{\boldsymbol{x}}$ in the a orientation [17]. He considered the motion of a membrane in shear, and argued that only the confined fluid relaxation mode ($m = 2$) is relevant for wavelengths less than L_p[32]:

$$\partial_t h + \dot{\gamma} y \partial_x h = \Lambda_0 \nabla^2 \frac{\delta\mathcal{H}}{\delta h} + \xi(\boldsymbol{x},t). \tag{2.12}$$

The linearity of the advection term leads to an analytic form for the height correlation that decreases with shear. Ramaswamy demonstrated that at a critical shear rate

$$\dot{\gamma}_c = \frac{T^3}{\kappa^2\eta\ell^3} \tag{2.13}$$

the fluctuations are significantly suppressed, provoking a layer collapse. Experimental confirmation of this was subsequently reported by Alkahwaji and Kellay [18]. Many other studies have incorporated the simple advection term in the dynamics for u: for example, Cates and Milner studied the effect of flow on the isotropic-lamellar transition [19], and Fredrickson studied the effect of flow on diblock lamellar phases [20]. All of these treatments are suitable if flow does not significantly perturb the layer microstructure. In contrast the perturbation of the microstructure in thermotropic lamellar phases was studied in Ref. [6]. In this case, shear flow was shown to introduce a tilt in the layers of a smectic-A liquid crystal. This led to layer reorientation and the possibility of an instability.

2. Membrane in Flow in the c orientation; non-linear advection

Now we consider the effect of a shear field $\boldsymbol{v} = \dot{\gamma} z\hat{\boldsymbol{x}}$ on a fluctuating membrane in the lamellar phase in the c orientation (Fig. 3). If we affinely transform the membrane in a small time δt, the height field advects according to

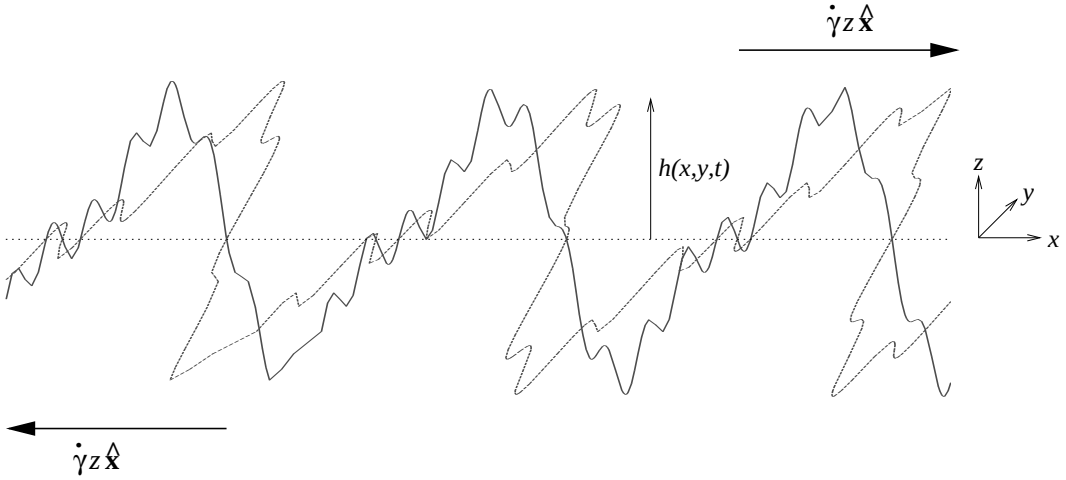

FIG. 3: A fluctuating membrane at rest (solid line) and subject to a shear field (dashed line).

$$h(x,y,t+\delta t) = h(x-\dot{\gamma} z \delta t, y, t) \qquad \Longrightarrow \qquad \frac{\partial h}{\partial t}\delta t = \frac{\partial h}{\partial x}(-\dot{\gamma} z \delta t) + \mathcal{O}(\delta t)^2. \tag{2.14}$$

The key point is that, because shear is assumed to advect the membrane, z should be equal to the height field h. This leads to a non-linear advective term, so that the equation of motion for a membrane in $(d-1)$ dimensions becomes:

$$\left[\partial_t + \dot{\gamma} h\left(\boldsymbol{x},t\right)\frac{\partial}{\partial x}\right] h(\boldsymbol{x},t) = -\int d^{d-1}x' \Lambda\left(\boldsymbol{x}-\boldsymbol{x}'\right)\frac{\delta \mathcal{H}}{\delta h(\boldsymbol{x}',t)} + \xi(\boldsymbol{x},t) \tag{2.15a}$$

$$-i\omega h(\boldsymbol{q},\omega) + i\dot{\gamma}\sum_{\Omega}\sum_{\boldsymbol{k}}(q_x - k_x)h(\boldsymbol{k},\Omega)h(\boldsymbol{q}-\boldsymbol{k},\omega-\Omega) = -\Lambda(\boldsymbol{q})\kappa q^4 h(\boldsymbol{q}) + \xi(\boldsymbol{q},\omega). \tag{2.15b}$$

The advective term stretches the membrane, leading to a restoring "tension". In contrast, the relevant advective term for a thermotropic in the c orientation remains $y\partial u/\partial x$, because the perturbation of the membrane structure is negligible, and undulations of u are always presumed to be of much smaller wavelength than the layer spacing. The noise has variance

$$\langle \xi(\boldsymbol{x}_1,t_1)\xi(\boldsymbol{x}_2,t_2)\rangle = D(\boldsymbol{x}_1-\boldsymbol{x}_2)\delta\left(\boldsymbol{x}_1-\boldsymbol{x}_2\right)\delta\left(t_1-t_2\right) \tag{2.16a}$$

$$\langle \xi(\boldsymbol{q}_1,\omega_1)\xi(\boldsymbol{q}_2,\omega_2)\rangle = D(\boldsymbol{q}_1)\delta^{d-1}(\boldsymbol{q}_1+\boldsymbol{q}_2)\delta(\omega_1+\omega_2) \tag{2.16b}$$

$$D(\boldsymbol{q}) = 2T\Lambda(\boldsymbol{q}) = 2T\Lambda_0|\boldsymbol{q}|^m \tag{2.16c}$$

$$\equiv D_0|\boldsymbol{q}|^m, \tag{2.16d}$$

where Eq. (2.16c) is the Fluctuation Dissipation Theorem.

A similar equation was derived for a diffuse interface between phase separated domains subject to shear by Bray and co-workers [10, 11]. However, there are two important differences. First, the "interface" of a membrane in the lamellar phase is intrinsically sharp. Second, although both bending ($\sim q^4$) and surface ($\sim q^2$) energies are present for a diffuse interface, at long length scales only the latter is relevant. On the other hand, surface tension is not present *a priori* in equilibrium lamellar phases, so the Helfrich Hamiltonian is dominated by the bending energy.

For no flow $\dot{\gamma} = 0$, the non-linear term in Eq. (2.15b) vanishes and

$$h(\boldsymbol{q},\omega) = G(\boldsymbol{q},\omega)\xi(\boldsymbol{q},\omega). \tag{2.17}$$

This defines the bare linear propagator, equivalent to the linearized equation of motion,

$$G^{-1}(\boldsymbol{q},\omega) = -i\omega + \Lambda(\boldsymbol{q})S^{-1}(\boldsymbol{q}), \tag{2.18}$$

where $S^{-1}(\boldsymbol{q}) = \kappa|\boldsymbol{q}|^4$. The poles of $G(\boldsymbol{q},\omega)$ yield the dispersion relation for the decay times of height fluctuations. The equal time height correlation function may be calculated from

$$C(\boldsymbol{q}) = \int_{-\infty}^{\infty}\frac{d\omega}{2\pi}C(\boldsymbol{q},\omega) \tag{2.19a}$$

$$= \int_{-\infty}^{\infty}\frac{d\omega}{2\pi}\langle h^*(\boldsymbol{q},\omega)h(\boldsymbol{q},\omega)\rangle \tag{2.19b}$$

$$= TS(\boldsymbol{q}). \tag{2.19c}$$

Equations (2.15b, 2.16b, 2.16d) define our model, with $\Lambda(\boldsymbol{q})$ given by Eq. (2.8). In the next section we examine the effect of the non-linear advective coupling on the spectrum of height fluctuations, through its effect on the linear propagator.

III. COARSE-GRAINING PROCEDURE

A. Description of the problem

We wish to calculate the effective dynamical response of the height field, determined by Eq. (2.15b), for different models specified by the relaxation function $\Lambda(\boldsymbol{q})$ and hence m. In Section III B below we show that a one-loop perturbation analysis leads to a divergent response for all candidate values for m. In order to avoid this unphysical divergence we apply a Renormalization Group (RG) procedure in Section III C to coarse-grain the system by removing the small scale and faster degrees of freedom, leaving an effective long wavelength theory. This procedure naturally generates a dynamic response that scales as q_x^2 due to the advective non-linearity, is suggestive of a tension, and restores non-singular behaviour.

In the study of dynamical critical phenomena [21] the description of a system is coarse-grained until fixed points are found for which the system is self similar. Hence, a condition is found on the parameters of the dynamical equations of motion that leaves the dynamics of the height field, scale invariant. Contrary to a system at its critical point, the lamellar system here can only be coarse-grained up to the natural physical cutoff of the collision length. However, since this length is not necessarily in the scaling regime, such a calculation requires detailed knowledge of the flow equations for all new terms generated in the equation of motion, which is generally impossible. On the other hand, if the collision length is close to, or larger than, the wavelength at which the scaling regime applies, we may use the simpler fixed point calculation as a guideline to estimate the effective long wavelength dynamics. In fact, even if we are not in the scaling regime, the other terms generated by coarse-graining are of higher order in wave vector and are irrelevant at the fixed point, and are thus in the process of being driven to zero during the coarse-graining procedure. In the hydrodynamic limit such terms are neglected.

In the following analysis, we coarse-grain the system to generate the lowest order (in wave vector) additional term in the equation of motion, which depends on the coarse-graining length L_p and the particular relaxation mechanism $\Lambda(\boldsymbol{q})$, parametrized by m. However, unless the appropriate range for the length scales of a given relaxation mechanism (see Fig. 2) encompasses the entire coarse-graining range, a full calculation demands a more precise choice of $\Lambda(\boldsymbol{q})$. We shall not attempt such a calculation, but give the results under the assumption that a single value of m applies throughout the wave vector regime of interest.

A consequence of the particular energy ($\sim q^2$) intrinsic to a diffuse interface is that Bray and co-workers were able to extract results only for "models" $m \geq 0$. In comparison, for a fluctuating membrane ($\sim q^4$), we may examine the relaxation mechanisms $m \geq -2$ including the case of an isolated impermeable membrane that relaxes by the hydrodynamic interaction of the surrounding solvent.

B. One-loop correction to $G(\boldsymbol{q},\omega)$

We start by rewriting Eq. (2.15b) as

$$h(\boldsymbol{q},\omega) = G(\boldsymbol{q},\omega)\left[\xi(\boldsymbol{q},\omega) - i\dot{\gamma}\sum_{\Omega}\sum_{\boldsymbol{k}}(q_x - k_x)h(\boldsymbol{k},\Omega)h(\boldsymbol{q}-\boldsymbol{k},\omega-\Omega)\right]. \tag{3.1}$$

Eq. (3.1) is shown in Fig. 4(a). Adding a perturbation $f(\boldsymbol{q},\omega)$ to Eq. (3.1) and averaging over the stochastic noise ξ results in a renormalized linear propagator G_R, defined by

$$G_R(\boldsymbol{q},\omega) = \lim_{f\to 0}\frac{\partial\langle h(\boldsymbol{q},\omega)\rangle}{\partial f(\boldsymbol{q},\omega)}, \tag{3.2}$$

given by the Dyson equation (Fig. 4b) [22],

$$G_R(\boldsymbol{q},\omega)^{-1} = G(\boldsymbol{q},\omega)^{-1} - \Sigma(\boldsymbol{q},\omega). \tag{3.3}$$

The self energy $\Sigma(\boldsymbol{q},\omega)$ shifts the poles of the effective propagator G_R and equivalently renormalizes the effective equation of motion (Eq. 2.18) for the long wavelength degrees of freedom. The one-loop contribution to the self energy $\Sigma(\boldsymbol{q},\omega)$ (Fig. 4c) yields

$$\begin{aligned}\Sigma(\boldsymbol{q},\omega) = -\dot{\gamma}^2\sum_{\Omega}\sum_{\boldsymbol{k}}(q_x - k_x)G(\boldsymbol{k},\Omega)G(\boldsymbol{q}-\boldsymbol{k},\omega-\Omega)\\ \times\Big[(q_x - k_x)G(-\boldsymbol{k},-\Omega)D(\boldsymbol{k}) + k_x G(\boldsymbol{k}-\boldsymbol{q},\Omega-\omega)D(\boldsymbol{k}-\boldsymbol{q})\Big].\end{aligned} \tag{3.4}$$

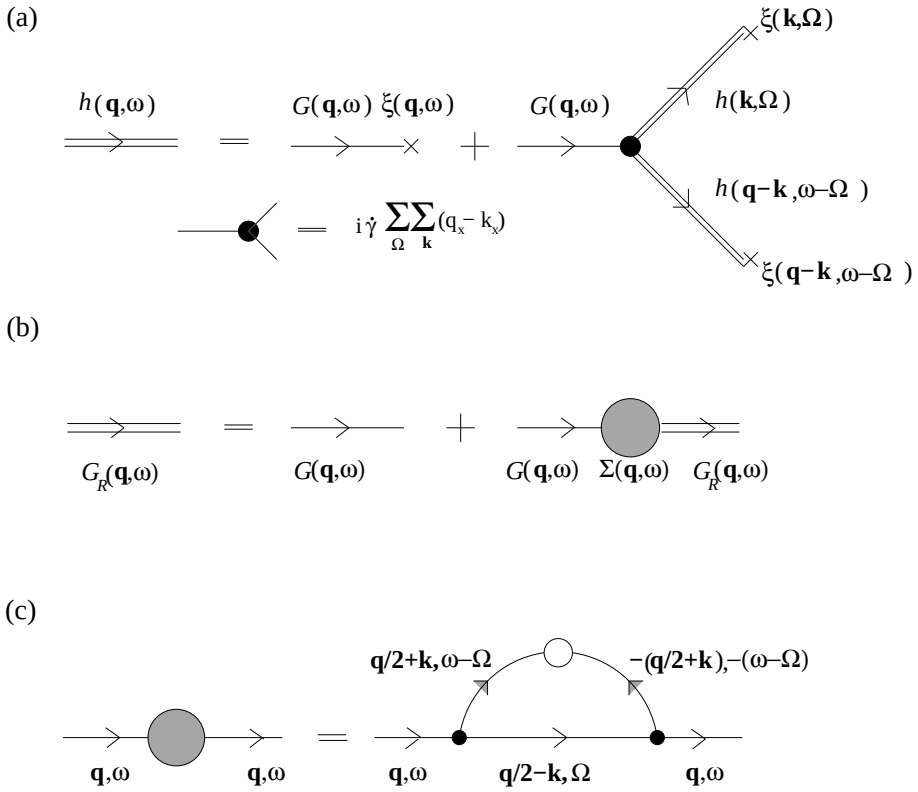

FIG. 4: (a) Diagrammatic representation of Eq. (3.1). Solid circles • represent non-linear vertices. (b) Dyson Equation for the renormalized propagator in terms of the bare propagator (single lines) and the self-energy (shaded circle). (c) One-loop correction to the self-energy. Open circles ∘ represent noise contractions, $\langle \xi\xi \rangle$.

A change of co-ordinates $\boldsymbol{k} \to \boldsymbol{q}/2 + \boldsymbol{k}$ and $\boldsymbol{k} \to \boldsymbol{q}/2 - \boldsymbol{k}$ in the first and second terms respectively of Eq. (3.4) gives

$$\Sigma(\boldsymbol{q},\omega) = -\dot{\gamma}^2 \sum_{\Omega} \sum_{\boldsymbol{k}} q_x \left(\frac{q_x}{2} - k_x\right) G\left(\frac{\boldsymbol{q}}{2} - \boldsymbol{k}, \Omega\right) \left| G\left(\frac{\boldsymbol{q}}{2} + \boldsymbol{k}, \omega - \Omega\right)\right|^2 D_0 \left|\frac{\boldsymbol{q}}{2} + \boldsymbol{k}\right|^m, \tag{3.5}$$

shown in Fig. 4. On symmetry grounds, the self energy can be written as

$$\Sigma(\boldsymbol{q},\omega) = a_2(\boldsymbol{q},\omega) q_x^2 + a_4(\boldsymbol{q},\omega) q_x^4 + \ldots, \tag{3.6}$$

in which case the renormalized propagator is given by

$$G_R(\boldsymbol{q},\omega)^{-1} \simeq -i\omega + \Lambda(\boldsymbol{q}) S^{-1}(\boldsymbol{q}) + a_2(\boldsymbol{q},\omega) q_x^2. \tag{3.7}$$

and the associated noise correlation is

$$\langle \xi(\boldsymbol{q}_1,\omega_1)\xi(\boldsymbol{q}_2,\omega_2)\rangle = \big(D(\boldsymbol{q}_1) + D_x q_x^2\big)\delta(\boldsymbol{q}_1 + \boldsymbol{q}_2)\delta(\omega_1 + \omega_2). \tag{3.8}$$

The effect of fluctuations on the slow hydrodynamic regime is due to the leading long wavelength static behavior, $\omega = 0$. Hence, we expand to order q_x^2 for $\omega \to 0$. Note that we implicitly ignore renormalizations of the frequency dependence, which should be sufficient to obtain scaling relations.

After converting the sum to a continuum integral and integrating out the frequency Ω (Eq. B5 in Appendix B), the lowest order term in q_x that appears in the static self-energy is

$$\Sigma(\boldsymbol{q},0) = -\dot{\gamma}^2 q_x^2 \frac{D_0}{2(\kappa\Lambda_0)^2} \int_0^\infty \frac{k^{d-2} dk S_{d-1}}{(2\pi)^{d-1}} \left[\frac{1}{4|\boldsymbol{k}|^{8+m}} + \frac{2k_x(k_x^3 + k_x k_\perp^2)}{2|\boldsymbol{k}|^{12+m}}\right] + \mathcal{O}(q_x^4), \tag{3.9}$$

where S_{d-1} is the unit sphere surface area in $(d-1)$ dimensions. For $10 + m - d > 0$, which encompasses all of our relaxation regimes $m = -1, 0, 2$, this integral di-

verges. In fact, before changing the limits of integration in Eq. (3.4), the divergence in Eq. (3.4) can be traced to the second term in square brackets at $\boldsymbol{q} = \boldsymbol{k}$. That is, the divergence is actually independent of the lower cutoff. Such a singular response suggests that a description in terms of the microscopic degrees of freedom is physically inconsistent. To proceed, we note that a tension-like term $\Lambda_x q_x^2$ added to the propagator yields non-singular behavior (Eq. B7 in Appendix B). Furthermore, we will show below that the gradual thinning of degrees of freedom during coarse-graining directly generates terms that render the response physical (Eq. B8 in Appendix B). Hence, we argue that the correct physical description of the highly fluctuating system in shear must formally be derived by projecting out the small scale degrees of freedom. We will outline this procedure next.

C. Renormalization Group (RG) analysis

Our goal is to successively "integrate out" the small scale fast degrees of freedom from the equation of motion, to yield an effective equation of motion for the remaining long wavelength degrees of freedom [23]. Schematically, we can write

$$h(\boldsymbol{x}, t) = h^{>}(\boldsymbol{x}, t) + h^{<}(\boldsymbol{x}, t), \tag{3.10}$$

where $h^{<}(\boldsymbol{x}, t)$ and $h^{>}(\boldsymbol{x}, t)$ are, respectively, small and large wave vector degrees of freedom. Upon removing the faster $h^{>}(\boldsymbol{x}, t)$, an effective equation of motion for $h^{<}(\boldsymbol{x}, t)$ will be generated. The form of the equation will differ from the original equation because of the non-linear advective term, which couples different modes together. Note that, generally, there are also non-linear terms (of order h^3) due to deviations from the Monge gauge limit and higher order advection terms, but the restriction of transverse length scales to within a patch length ensures that we remain close to this limit. The new equation of motion is most easily cast in terms of the renormalized propagator $G_R^{<}$ of the long wavelength degrees of freedom. As noted above, we expect the contributions to the propagator, and generally to the noise, to be even powers in q_x^2, because of the symmetry of the non-linearity. In the hydrodynamic and long wavelength limit, and indeed because higher order terms are irrelevant at the non-trivial fixed point, we focus on corrections of order q_x^2.

Essentially there are three steps to a momentum-shell RG in which, for convenience, we impose a short wavelength ultraviolet cutoff λ in the x-direction only; these are the fluctuations directly suppressed by flow. Physically, the original cutoff is $\lambda = \pi/a$, where a is of order a molecular (surfactant) size, and we are interested in coarse-graining from this length to some, unknown, length, at which non-trivial scaling behavior is seen. The steps are as follows:

1. The first step is to divide the Brillouin zone $k \in [0, \lambda]$ into two parts: high wave vectors $k^{>} \in [\lambda/b, \lambda]$ to be removed, and the remaining long wavelengths $k^{<} \in [0, \lambda/b]$. The elimination of (assumed) fast modes results in an effective renormalized propagator $G_R^{<}(\boldsymbol{q}, \omega)$. Since there are no singularities in this range of integration, only finite corrections to the parameters result.

2. After coarse-graining, the resulting equation has a cutoff λ/b. This difference from the original model is removed by rescaling the length scales, x, $x_\perp$, h and the time scale t.

3. Finally we look for the fixed points of the recursion relation at which the theory is invariant under the first two steps.

This procedure generates a recursion equation that may be used to find the behavior of the system in a scaling regime. Generally, this scaling regime corresponds to a description of the system at wavelengths longer than that wavelength at which the dynamics has effectively been driven to the fixed point. We will use this fixed point as an *estimate* of the dynamics of the system at wavelengths larger than the collision length L_p.

We follow Bray *et al.'s* study [10, 11] of the influence of shear flow on interfacial dynamics in a phase separating system, which is governed by square gradient terms rather than quartic energy possessed by membranes. The scale transformation takes the form

$$x = bx', \qquad \boldsymbol{x}_\perp = b^\zeta \boldsymbol{x}'_\perp, \qquad h = b^\chi h', \qquad t = b^z t'. \tag{3.11}$$

Since shear suppresses the fluctuations in the x-direction we expect to find $\zeta \leq 1$ when the shear is relevant. We will see that condition is only satisfied if $m \geq -2$. Since we consider only models $m \geq -1$, this condition is always satisfied. In such cases the transverse part $\boldsymbol{q}_\perp$ dominates q_x in the terms involving powers of $|\boldsymbol{q}|$ so that the bare propagator is renormalized to

$$G_R^{-1}(\boldsymbol{q}, \omega) = -i\omega + \Lambda(\boldsymbol{q}_\perp) S^{-1}(\boldsymbol{q}_\perp) + \Lambda_x q_x^2, \tag{3.12}$$

and the noise correlator is

$$\langle \xi(\boldsymbol{q}_1, \omega_1) \xi(\boldsymbol{q}_2, \omega_2) \rangle = \big(D(\boldsymbol{q}_{1\perp}) + D_x q_x^2 \big) \delta(\boldsymbol{q}_1 + \boldsymbol{q}_2) \delta(\omega_1 + \omega_2). \tag{3.13}$$

We have included the lowest order correction to G_R and the noise from the non-linearity. Applying the rescaling

Eq. (3.11) yields rescaled parameters in the equation of motion and the noise correlator:

$$\dot{\gamma}' = b^{\chi+z-1}\dot{\gamma} \tag{3.14a}$$
$$\Lambda' = b^{z-(4+m)\zeta}\Lambda \tag{3.14b}$$
$$\Lambda'_x = b^{z-2}\Lambda_x + \dots \tag{3.14c}$$
$$D'_0 = b^{z-2\chi-1-m\zeta-(d-2)}D_0 \tag{3.14d}$$
$$D'_x = b^{z-2\chi-3-(d-2)\zeta}D_x + \dots \tag{3.14e}$$

The parameters Λ'_x and D'_x acquire perturbative corrections due to the coarse-graining step of the RG procedure. In contrast $\dot{\gamma}$, Λ and D_0 do not acquire perturbative corrections. The nonrenormalizability of $\dot{\gamma}$ follows from Galilean invariance of Eq. (2.14), which transforms $t \to t + \delta t$ and $x \to x - \dot{\gamma} h \delta t$ in the equation of motion.

We first examine the linear theory to identify the critical dimension d_c. Since there are no perturbative corrections to a linear theory, the requirement that the exponents for b vanish in Eqs. (3.14b-3.14e) yields the conditions

$$z_0 = 2, \qquad \zeta_0 = \frac{2}{m+4}, \qquad \chi_0 = \frac{8-m-2d}{2(m+4)}. \tag{3.15}$$

The subscripts denote the application to the linear theory. Eq. (3.14a) determines the relevance of the shear rate $\dot{\gamma}$ on the coarse-graining, at the trivial fixed point. From Eq. (3.15) we obtain $\chi_0 + z_0 - 1 = (m - 2d + 16)/[2(4+m)]$. Therefore, $\dot{\gamma}$ is relevant for $d < d_c$ where

$$d_c = \frac{16+m}{2}, \qquad m \geq -2. \tag{3.16}$$

We can coarse-grain the theory perturbatively in Fourier space near the critical dimension d_c of the theory. For $d < d_c$ we expect a new fixed point to appear at which $\dot{\gamma}$, Λ and D_0 are non-zero. Eqs. (3.14a, 3.14b, 3.14d) give the corresponding exponents exactly,

$$z = \frac{3(4+m)}{14+2m-d}, \quad \zeta = \frac{3}{14+2m-d}, \quad \chi = \frac{8-m-2d}{2(4+m)}. \tag{3.17}$$

From Eqs. (3.15) and (3.17) we see that $\zeta \leq 1$ for $m \geq -2$, in which case the approximation $|\boldsymbol{q}| \sim |\boldsymbol{q}_\perp|$ is consistent. From Eq. (3.17) we find $D'_x = b^{-8/(4+m)}D_x$, indicating that D_x flows to zero at the fixed point (Fig. 5).

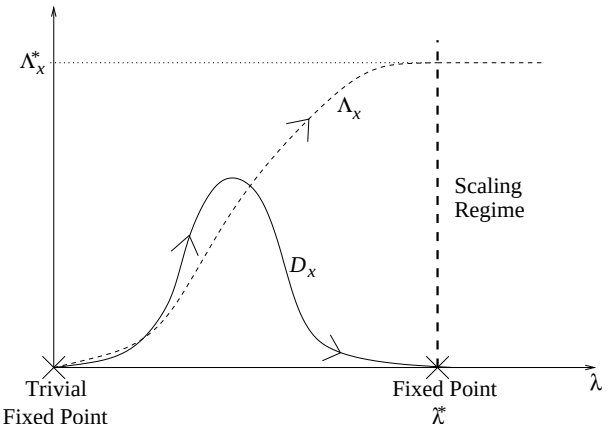

FIG. 5: Schematic flows of Λ_x and D_x as a function of the coarse-graining length λ.

To find the values of Λ_x and λ at the non-trivial fixed point we now return to the RG procedure. Integrating Eq. (3.3) over the short wavelength modes gives the equation for the effective renormalized propagator

$$G_R^<(\boldsymbol{q},\omega)^{-1} = G(\boldsymbol{q},\omega)^{-1} - \Sigma(\boldsymbol{q},\omega), \tag{3.18}$$

where $\Sigma(\boldsymbol{q},\omega)$ is given in Eq. (3.5). Then, setting $b = e^l$ with l infinitesimal, Eqs. (3.14c) and (3.18) generate a differential flow equation for Λ_x

$$\frac{d\Lambda_x}{dl} = \Lambda_x \left[(z-2) - \lim_{\boldsymbol{q}\to 0} \frac{1}{\Lambda_x q_x^2 l}\Sigma(\boldsymbol{q},0) \right]. \tag{3.19}$$

Step (3) of the RG analysis consists of finding the fixed points Λ_x^* for which the theory is invariant. This procedure is carried out in Appendix B for each value of m. Finally, we can make contact with our original discussion of an induced "tension" σ, and extract a tension according to Eq. (1.3). The results are collected in Table I. For $m = 0$ and $m = 2$ the procedure is straightforward and the results (and Λ_x) are independent of the low-k cutoff of the theory. However, for $m = -1$ we must cut off the theory at $k = \pi/L_p$, and hence we find a result for Λ_x that depends on L_p.

As noted in the introduction, on the basis of estimating the height correlation function from the first term in the perturbation expansion in Eq. (3.1), we would naively expect the "tension" to scale quadratically with the strain rate; this scaling was also captured by considering the energetic cost of bending and stretching a single membrane [8]. However, an anomalous scaling $\Lambda_x \sim \dot{\gamma}^{\varepsilon_m}, \varepsilon_m \neq 2$ is generated in the scaling regime for $m = 0$ and $m = 2$. The case of $m = -1$ is different. Owing to the divergence in the perpendicular direction at the low cutoff due to the more violent fluctuations at long wavelengths, the scaling does not follow the expected pattern ($\varepsilon_{-1} = 2/3$) of the

other mechanisms. However, whether accidentally or not, the first term in its power series satisfies $\varepsilon_{-1} = 2$ so at low strain rates it cannot be considered to exhibit anomalous scaling; in general though, contributions from higher order terms indicate that the scaling is also anomalous.

In addition, equating bending and tension energies leads to an expression for the shear rate $\dot{\gamma}_c$ at which fluctuations are significantly suppressed,

$$\dot{\gamma}_c \sim \frac{T^{(m+3)/2}\Lambda_0}{\kappa^{(m+1)/2}\ell^{m+4}}, \tag{3.20}$$

where in the case $m = -1$ there are higher order contributions, shown in Table I. If we compare the critical shear rate for isolated impermeable membrane relaxation with Bruinsma's result (Eq. 2.11), the scaling is the same apart from a factor of $\sqrt{T/\kappa}$.

D. One-Step Coarse-Graining

So far we have demonstrated how to calculate the nontrivial scaling behavior of the membrane, assuming that fluctuations generate a tension-like term that renders contributions to the self-energy non-singular. Here, we show explicitly how the "first step" of a coarse-graining procedure produces such a term. Here we coarse-grain the system in "one step", by making a small perturbation to the original microscopic cutoff $\lambda = \pi/a$, where a is a typical molecular dimension. For a small perturbation about the trivial fixed point ($\Lambda_x = 0$) the differential flow equation Eq. (3.19) becomes

$$d\Lambda_x \simeq -\lim_{\boldsymbol{q}\to 0} \frac{1}{q_x^2}\Sigma(\boldsymbol{q}, 0). \tag{3.21}$$

We show at the end of Appendix B the calculation of the coarse-grained self-energy in the limit $\Lambda_x \to 0$ (Eq. B20). Inserting the resulting self-energy (Eq. B21) into the recursion relation yields an expression for Λ_x and, via Eq. (1.3), a "tension" that depends on the cutoff and the relaxation mechanism,

$$\sigma = \beta \frac{T}{\kappa^2\Lambda_0^2\lambda^{9+m-d}}\dot{\gamma}^2 l q^{-m}, \tag{3.22}$$

where β is a numerical prefactor and l is a small number that depends on the chosen coarse-graining step. As expected, for all relaxation mechanisms, a first step coarse-graining leads to a "tension" that is the same as the naive scaling $\sim \eta^2\dot{\gamma}^2$. Thus we may infer that the coarse-graining process modifies the dependence of the scaling for $m = 0, m = 2$ and also for $m = -1$ (but not for very small strain rates).

IV. RESULTS AND DISCUSSION

A. Single Membrane Dynamics in the Scaling Regime

We have considered the dynamics of a single membrane in the c-orientation (Fig. 1) with respect to shear flow. Advection couples different Fourier modes, and hence renormalizes the effective response. We have estimated the effective long-wavelength theory, that would be obtained by removing smaller and faster degrees of freedom with wave vectors $q > \lambda$, by calculating the behavior of the fluctuating membrane in the scaling regime. This dynamic coarse-graining generates, to lowest order, a term $-\Lambda_x q_x^2$ in the long wavelength propagator. This is the principle qualitative result of this work.

The function Λ_x depends on wave vector q, the quiescent relaxation mechanism $\Lambda(\boldsymbol{q})$, the strain rate, and the wavector scale λ to which coarse-graining has been performed (Appendix B):

$$\Lambda_x \sim A_m \lambda^{\delta_m}\dot{\gamma}^{\varepsilon_m} \tag{4.1}$$

where m parametrizes the relaxation mechanism $\Lambda(\boldsymbol{q}) = \Lambda_0 q^m$, and the constant A_m depends on T, κ, L_p, and Λ_0. The results are summarized in Table I. This restoring term is suggestive of an anisotropic "tension" σ, which would appear in the dynamics as $\sigma q_x^2 h^<(\boldsymbol{q})$ (Eq. 1.3), with $\sigma = \Lambda_x/\Lambda(\boldsymbol{q})$, except that the non-analytic form generally leads to a wave vector dependence. In the permeable limit the wavector dependence is absent, $\nu = 0$, while in other cases there is a wave vector dependence. Hence, referring to the newly generated term as a tension is suggestive at best. Nonetheless, this term can be expected to suppress fluctuations, and hence influence the effective collision rate, and in turn the Helfrich interaction potential, in the presence of shear flow. Elsewhere, we have used an effective energetic tension to parametrize the reduction in fluctuations and the corresponding flow-induced strain or change in layer spacing [7].

It is important to recognize that, although the "tension" in Table I applies, strictly, only to wavelengths of order the collision length, it is generated at all wavelengths larger than the smallest cutoff and grows during the coarse-graining procedure. In reference [7] we replaced this wavevector-dependent tension by an average value that applies for all wave vectors. This certainly changes any quantitative predictions, but does not influence the qualitative aspects of those results. This naive estimate should evidently be replaced by a much more sophisticated dynamic analysis that simultaneously performs the dynamic coarse-graining in the presence of the advective non-linearity and a self-consistent (or coarse-graining) procedure to recover the Helfrich interaction behavior that stabilizes the lamellar stack. Such a calculation is beyond the scope of this work.

If the layer spacing *does* adjust in flow due to an induced tension, a non-Newtonian response is likely to be

TABLE I: Row (2) shows the fixed points corresponding to different membrane relaxation mechanisms, given in row (1). Row (3) gives the "tension", defined by Eq. (1.3) as a function of the cutoff, λ and the relaxation mechanism. Rows (4) and (5) display the results for $\lambda^{-1} \sim L_p$ and $q^{-1} \sim L_p \sim \ell\sqrt{\kappa/T}$ respectively. Row (6) displays the critical shear rate for suppression of fluctuations.

	Membrane	Isolated ($m=-1$)	Permeable ($m=0$)	Confined ($m=2$)
(1)	$\Lambda(\boldsymbol{q}) = \Lambda_0 q^m$	$\frac{1}{\eta q}$	$\frac{\zeta q^0}{\eta}$	$\frac{d^3 q^2}{\eta}$
(2)	$\Lambda_x^*(\lambda, \Lambda_0)$	$\alpha_0 \frac{T\lambda L_p^6}{\Lambda_0 \kappa^2}\dot{\gamma}^2 + \mathcal{O}(\dot{\gamma}^4)$	$\alpha_1 \frac{T^{4/11}\Lambda_0^{3/11}}{\kappa^{1/11}\lambda^{10/11}}\dot{\gamma}^{8/11}$	$\alpha_3 \frac{T^{2/5}\Lambda_0^{4/5}}{\kappa^{1/5}\lambda^{4/5}}\dot{\gamma}^{4/5}$
(3)	$\sigma(\lambda, \Lambda_0, q)$	$\alpha_0 \frac{T\lambda L_p^6}{\Lambda_0^2 \kappa^2}\dot{\gamma}^2 q + \mathcal{O}(\dot{\gamma}^4)$	$\alpha_1 \frac{T^{4/11}}{\kappa^{1/11}\Lambda_0^{8/11}\lambda^{10/11}}\dot{\gamma}^{8/11} q^0$	$\alpha_3 \frac{T^{2/5}}{\kappa^{1/5}\Lambda_0^{4/5}\lambda^{4/5}}\dot{\gamma}^{4/5} q^{-2}$
(4)	$\sigma(L_p, q)$	$\alpha_0 \frac{TL_p^5}{\kappa^2}\eta^2\dot{\gamma}^2 q + \mathcal{O}(\dot{\gamma}^4)$	$\alpha_1 \frac{T^{4/11}}{\kappa^{1/11}} \frac{L_p^{10/11}}{\zeta^{8/11}}\eta^{8/11}\dot{\gamma}^{8/11} q^0$	$\alpha_3 \frac{T^{2/5}}{\kappa^{1/5}} \frac{L_p^{2/5}}{d^{12/5}}\eta^{4/5}\dot{\gamma}^{4/5} q^{-2}$
(5)	$\sigma(d)$	$\alpha_0 \frac{\ell^4}{T}\eta^2\dot{\gamma}^2 + \mathcal{O}(\dot{\gamma}^4)$	$\alpha_1 \frac{\kappa^{4/11}}{T^{1/11}} \frac{\ell^{10/11}}{\zeta^{8/11}}\eta^{8/11}\dot{\gamma}^{8/11}$	$\alpha_3 \frac{\kappa^{6/5}}{T}\ell^{2/5}\eta^{4/5}\dot{\gamma}^{4/5}$
(6)	$\dot{\gamma}_c$	$\frac{T}{\eta\ell^3}\left(1 - \frac{1}{2}\left(\frac{T}{\eta\ell^3}\right)^2 + \dots\right)$	$\frac{T^{3/2}\zeta}{\kappa^{1/2}\eta\ell^4}$	$\frac{T^{5/2}}{\kappa^{3/2}\eta\ell^3}$

found. Most probably this will be shear thinning, because of the greater local regularity of the flow, although it is not obvious that this is the case. The magnitude of the viscous response is a complicated balance of dissipation incurred within bilayers, and local inhomogeneous shears due to the fluctuating layers. The single study that reported a change in layer spacing also reported a shear thinning response [4]. Shear thinning behaviour has been observed in some Helfrich-stabilized systems including $C_{12}E_5$ [4], AOT [24] and SDS [25].

B. Effective Long Wavelength Dynamics

The effective long wavelength dynamics of the single membrane is of the form (in Fourier space)

$$-i\omega h^<(\boldsymbol{q},\omega) + i\dot{\gamma}\sum_{\Omega}\sum_{\boldsymbol{k}}(q_x - k_x)h^<(\boldsymbol{k},\Omega)h^<(\boldsymbol{q}-\boldsymbol{k},\omega-\Omega) = -\left[\Lambda(\boldsymbol{q})\kappa q^4 + \Lambda_x q_x^2\right]h^<(\boldsymbol{q}) + \xi^<(\boldsymbol{q},\omega), \tag{4.2a}$$

$$\langle \xi^<(\boldsymbol{q}_1,\omega_1)\,\xi^<(\boldsymbol{q}_2,\omega_2)\rangle = (D(\boldsymbol{q}_1) + D_x q_x^2)\delta(\boldsymbol{q}_1+\boldsymbol{q}_2)\delta(\omega_1+\omega_2), \tag{4.2b}$$

where $h^<(\boldsymbol{q},\omega)$ is the small wave vector (coarse-grained) height field, and the noise $\xi^<$, in principle, incorporates the eliminated degrees of freedom in addition to the original small scale degrees of freedom. This yields a proportionality between correlation and response, and a generalized fluctuation-dissipation theorem (FDT) is satisfied, although the simple proportionality factor of temperature relating correlation and response is replaced by the more complicated noise correlations. In the case, which we have assumed, that the scaling limit is reached before the patch size has been reached, D_x vanishes and an effective temperature, albeit shear rate dependent, can be ascribed to the system according to the fixed point value for D.

Ideally, coarse-graining should continue until all wavelengths less than the collision length L_p have been removed, at which point the resulting theory would be used as a starting point for understanding the dynamics of the usual mean smectic layer displacement u, rather than the microscopic membrane position h. Note that, at this point, collisions

intervene in a non-trivial way to limit affine layer advection, and the coarse-grained smectic phase variable u advects according to $\dot{\gamma} y \partial_x u$ rather than $\dot{\gamma} u \partial_x u$. This behavior should, in principle, emerge smoothly in an ideal calculation.

The resulting dynamics of a strongly fluctuating layered system in shear flow are best cast in terms of the velocity field, in the standard two-fluid form [26], as

$$\rho \left(\partial_t + \boldsymbol{v} \cdot \boldsymbol{\nabla}\right) \boldsymbol{v} = -\boldsymbol{\nabla} p + \eta \nabla^2 \boldsymbol{v} + \hat{\boldsymbol{n}}\, f_n \tag{4.3}$$

$$\left(\partial_t + \boldsymbol{v} \cdot \boldsymbol{\nabla}\right) u = v_z, \tag{4.4}$$

where we have, for convenience, shown the form in the absence of permeation. The normal force f_n differs from the usual normal force by the term generated upon coarse-graining,

$$f_n = -\left[\frac{\delta \mathcal{F}}{\delta u(q,t)} + \frac{\Lambda_x \Lambda^{-1}(\boldsymbol{q})}{d} q_x^2 u(q,t)\right], \tag{4.5}$$

where the free energy $\mathcal{F}$ should also include the layer compression energy density $\frac{1}{2}\bar{B}\left(\partial_z u\right)^2$. Note the factor of d in the second term, reflecting the inherent three dimensional nature of smectic elasticity. The noise defines an effective temperature that is generally not the physical temperature, and may have additional correlations $D_x q_x^2$ that reflect the flow (depending on whether or not the scaling regime has been reached).

The additional term is only present for strong flows, and penalises layer undulations in the x direction; this is because such undulations are performed at the expense of the microscopic height fluctuations, which are highly stretched in strong flows. This term is *not* expected to appear in situations where the microstructure of the smectic layers is essentially undisturbed by flow, as in typical thermotropic smectics (but see the calculation of Auernhammer *et al.* [6] for a counter example). One could also envision this term as a non-equilibrium contribution to an effective free energy, which has been postulated by Jou and co-workers in their studies of complex fluids using extended irreversible thermodynamics [27]; however the dependence on strain rate that we derive, $\Lambda_x \sim \dot{\gamma}^{\varepsilon_m}$, is not necessarily analytic, unlike their assumptions.

It is important to remember that the generation of the tension-restoring term is only one of several possible dynamic effects; other effects include the rearrangement of defect distributions, which is also likely to lead to a shear thinning response [28].

C. Summary

In this work we have studied the effect of flow on the dynamics of fluctuating membranes. We have made several assumptions, which we collect for completeness:

- We assumed that an ε-expansion is sufficient to describe the effect of coarse-graining the theory up to the collision length; in this limit the renormalized noise reduces to an effective temperature. Whether or not scaling is truly reached is an open question. It is more likely that there are residual noise correlations when the collision length has been reached. Moreover, the critical dimension d_c is quite high and fluctuations are quite important; we have considered $m = -1, 0, 2$, for which, respectively, $d_c = \frac{15}{2}, 8, 9$.
- Since an ε-expansion is not likely to hold so far from the critical dimension, our calculation is strictly a self-consistent one-loop calculation.
- We have considered the different membrane relaxation mechanisms (permeable, squeezing, isolated) separately. In reality, the mechanism changes during the coarse-graining process, according to Fig. 2; nonetheless, this does not detract from our primary message, that the perturbation of the microstructure of highly fluctuating membranes can lead to an additional restoring term in the long wavelength dynamics.
- The coarse-graining can be performed only up to L_p, because at this length scale the long range steric repulsion is important. In fact, we have completely ignored steric interactions. A more precise treatment would involve simultaneously treating flow and collisions, or treating the flow within a self-consistent scheme using, for example, a harmonic potential to mimic collisions.

The significant accomplishments of this study have been, first, a qualitative estimate of the effect of flow on highly fluctuating lamellar phases. More importantly, however, is the demonstration that flow can strongly modify the fluctuation spectrum and generate new effects in the macroscopic response, via an RG-like self-consistent coarse-graining technique. The theory that emerges has a natural effective noise that need not satisfy the usual equilibrium fluctuation-dissipation theorem. Similar renormalizations of hydrodynamic descriptions can be expected for other complex fluid systems with highly fluctuating mesoscopic degrees of freedom, such as wormlike micellar systems (for example, the micellar length, modulus, and relaxation times could be ex-

pected to renormalize due to the effect of flow on the local charge distribution and undulation spectra).

Acknowledgments

We thank A. J. Bray for helpful advice.

APPENDIX A: PERMEATION LENGTH SCALE

We estimate the permeation length ζ by assuming that permeation is dominated by solvent flow through pores in the membranes; indeed, at certain surfactant concentrations pores are very common – see for example the studies [29, 30]. We assume cylindrical pores of diameter $2w$ within a membrane of thickness τ, separated by a mean distance R (Fig. 6). We wish to derive the kinetic coefficient Λ_0 for layer relaxation, defined by

$$\partial_t h = -\Lambda_0 \frac{\delta \mathcal{H}}{\delta h}. \tag{A1}$$

Identifying the mean solvent flow velocity $\langle v \rangle$ with the relaxation speed of the membrane $\partial_t h$ yields

$$\langle v \rangle \sim \Lambda_0 \frac{\delta \mathcal{H}}{\delta h}. \tag{A2}$$

The pressure difference $\Delta p = p^+ - p^-$ driving solvent flow is given by the force per area $\delta\mathcal{H}/\delta h$ that the membrane exerts on the fluid. Thus the kinetic coefficient is

$$\Lambda_0 \sim \frac{\langle v \rangle}{\Delta p}. \tag{A3}$$

For each pore the mean velocity is the flux of material Q flowing through a pore per unit surface area of membrane A,

$$\langle v \rangle = \frac{Q}{A}. \tag{A4}$$

We note that in terms of permeability $\mathcal{P}$, the flux is given by $Q/A = -\mathcal{P}\nabla p/\eta$ (Darcy's law). Thus $\mathcal{P} \simeq \Lambda_0 \eta \tau$, which was used by Leng [31] in the context of swelling compressed lamellar phases. To calculate the flux we assume that the pressure gradient sets up a Poiseuille flow given by the viscous flow force balance

$$\eta \frac{v_c}{w^2} \simeq \frac{\Delta p}{\tau} \tag{A5}$$

where v_c is the velocity of the solvent at the centre of the flow, and so

$$\frac{Q}{A} \sim \frac{w^4}{R^2 \tau} \frac{\Delta p}{\eta}. \tag{A6}$$

On substituting the expression for the mean velocity in Eq. (A3) by the flux in Eq. (A6) we obtain an expression for the kinetic coefficient

$$\Lambda_0 \sim \frac{w^4}{\tau R^2 \eta}. \tag{A7}$$

Therefore, the "permeation length" is $\zeta = w^4/(R^2\tau)$.

APPENDIX B: CALCULATION OF THE SELF-ENERGY AND THE CRITICAL POINTS FOR DIFFERENT RELAXATION MECHANISMS

In this appendix we calculate the coarse-grained self-energy $\Sigma(\boldsymbol{q}, 0)$, which we insert into the recursion relation (Eq. 3.19) to find the fixed points Λ_x^* for different values of m. We also calculate the general expression for the self-energy, and the associated Λ_x derived from the recursion relation in a "first step" coarse-graining process.

1. Coarse-grained self energy

After demonstrating that a naive calculation of the self-energy, equivalent to $\Lambda_x = 0$, leads to a divergence, the main task here is to show how the divergence is eliminated for $\Lambda_x \neq 0$, enabling us to proceed with the integration. Having established in Section III B that the self energy (Eq. 3.5) can be written in powers of q_x^2, we commence from its expression in terms of the renormalized propagator (Eq. 3.7) and its corresponding noise correlation (Eq. 3.8);

$$\Sigma(\boldsymbol{q}, \omega) = -\dot{\gamma}^2 \sum_{\Omega} \sum_{\boldsymbol{k}} q_x \left(\frac{q_x}{2} - k_x \right) G_R \left(\frac{\boldsymbol{q}}{2} - \boldsymbol{k}, \Omega \right) \left| G_R \left(\frac{\boldsymbol{q}}{2} + \boldsymbol{k}, \omega - \Omega \right) \right|^2 \left[D_0 \left| \frac{\boldsymbol{q}}{2} + \boldsymbol{k} \right|^m + D_x \left(\frac{q_x}{2} + k_x \right)^2 \right]. \tag{B1}$$

We consider the slow hydrodynamic regime $\omega \to 0$, and ignore frequency-dependent corrections, so that

$$G_R(\boldsymbol{q}, \omega)^{-1} \simeq -i\omega + \Lambda(\boldsymbol{q}) S^{-1}(\boldsymbol{q}) + \Lambda_x q_x^2, \tag{B2}$$

where $\Lambda_x \equiv a_2(\boldsymbol{q}, 0)$, $\Lambda(\boldsymbol{q}) = \Lambda_0 q^m$ and $S^{-1}(\boldsymbol{q}) = \kappa q^4$. The disregard for frequency-dependent corrections should suffice to obtain scaling properties. The sums are converted to integrals by Eq. (2.2)

$$\sum_{\Omega} \sum_{\boldsymbol{k}} \to \int \frac{d\Omega}{2\pi} \int_{\pi/L_p}^{\pi/a} \frac{d^{d-1} k S_{d-1}}{(2\pi)^{d-1}}, \tag{B3}$$

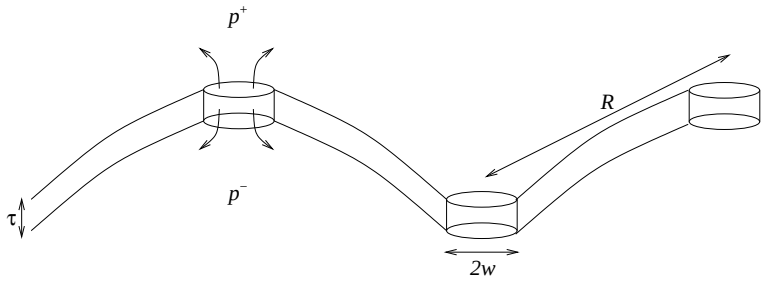

FIG. 6: Pore defects in a membrane (side view).

where $S_n = n\pi^{n/2}/\Gamma(n/2+1)$ is the surface area of an n dimensional unit sphere and the limits in $\boldsymbol{k}$ are given by the physical cutoffs. The first step is to perform the Ω-integral by contour integration, yielding a positive pole at $i\Omega = -\left[\Lambda_x\left(k_x+\frac{q_x}{2}\right)^2+\kappa\Lambda_0\left|\boldsymbol{k}+\frac{\boldsymbol{q}}{2}\right|^{4+m}\right]$,

$$\Sigma(\boldsymbol{q},0) = -\frac{\dot\gamma^2}{2}\int_0^\infty \frac{k^{d-2}dkS_{d-1}}{(2\pi)^{d-1}} \frac{q_x\left(\frac{q_x}{2}-k_x\right)\left[D_0\left|\boldsymbol{k}+\frac{\boldsymbol{q}}{2}\right|^m + D_x\left(k_x+\frac{q_x}{2}\right)^2\right]}{\left[\Lambda_x\left(k_x+\frac{q_x}{2}\right)^2+\kappa\Lambda_0\left|\boldsymbol{k}+\frac{\boldsymbol{q}}{2}\right|^{4+m}\right]\left[2\Lambda_x\left(k_x^2+\frac{q_x^2}{4}\right)+\kappa\Lambda_0\left|\boldsymbol{k}+\frac{\boldsymbol{q}}{2}\right|^{4+m}+\kappa\Lambda_0\left|\boldsymbol{k}-\frac{\boldsymbol{q}}{2}\right|^{4+m}\right]}. \tag{B4}$$

As we explained in Section III B, the leading long wavelength behaviour arises from an expansion of Eq. (B4) to lowest order in q_x^2, which we now investigate for the cases $\Lambda_x = 0$ and $\Lambda_x \neq 0$. For $\Lambda_x = 0$, and thus also $D_x = 0$, the self-energy becomes

$$\Sigma(\boldsymbol{q},0) = -\dot\gamma^2 q_x^2 \frac{D_0}{2(\kappa\Lambda_0)^2}\int_0^\infty \frac{k^{d-2}dkS_{d-1}}{(2\pi)^{d-1}}\left[\frac{1}{4|\boldsymbol{k}|^{8+m}}+\frac{2k_x(k_x^3+k_xk_\perp^2)}{2|\boldsymbol{k}|^{12+m}}\right]+\mathcal{O}(q_x^4), \tag{B5}$$

which diverges at low $\boldsymbol{k}$ for $10+m-d>0$ (note that all relaxation mechanisms we consider obey $m > d-10$). As we discuss at the end of Section III B, this divergence is unphysical. Upon coarse-graining the theory, the term $\Lambda_x q_x^2$ will be generated, which obviously changes the character of the integral. Next we show that the implementation of coarse-graining such that $\Lambda_x \neq 0$ removes this divergence.

Following the first step of the renormalization group analysis in Section III C the removal of high wave vectors $\boldsymbol{k}^>$ in the x direction in the range $\lambda e^{-l} < k_x < \lambda$ is equivalent to a change in limits,

$$\sum_{\boldsymbol{k}^>} \to \int_{\lambda e^{-l}}^{\lambda}\frac{dk_x}{2\pi}\int_0^\infty \frac{d^{d-2}k_\perp S_{d-2}}{(2\pi)^{d-2}}. \tag{B6}$$

Note that there is no change in the limits in the perpendicular direction. We showed in Section III C that when $\Lambda_x \neq 0$ and $m \geq -1$, we approximate $|\boldsymbol{k}| \to |\boldsymbol{k}_\perp|$ so that the renormalized propagator becomes Eq. (3.12) and the noise becomes Eq. (3.13). In addition, within the scaling regime or close to the fixed point, $D_x \to 0$. With these assumptions the resulting approximation to the lowest order expansion of the self energy is

$$\Sigma(\boldsymbol{q},0) = -\dot\gamma^2 q_x^2\frac{D_0}{2}\int_{\lambda e^{-l}}^{\lambda}\frac{dk_x}{2\pi}\int_0^\infty \frac{k_\perp^{d-3}dk_\perp S_{d-2}}{(2\pi)^{d-2}}.\frac{k_\perp^m}{\left(\Lambda_x k_x^2+\kappa\Lambda_0 k_\perp^{4+m}\right)^2}\left[\frac{1}{4}+\frac{\Lambda_x k_x^2}{2\left(\Lambda_x k_x^2+\kappa\Lambda_0 k_\perp^{4+m}\right)}\right]+\mathcal{O}(q_x^4). \tag{B7}$$

The divergence that we encountered before for $\Lambda_x = 0$ is now eliminated, which enables us to proceed with the integration over all wave vectors in the transverse direction, in order to calculate the self-energy $\Sigma(\boldsymbol{q},0)$ to be inserted into the recursion relation (Eq. 3.19).

2. Calculation of the fixed points

With the condition that $d+m-2>0$ (a criterion that we discuss later), integration of Eq. (B7) leads to

$$\Sigma(\boldsymbol{q},0) = -2\frac{(14+2m-d)}{m+10-d}U\Lambda_x q_x^2 l \qquad (d+m-2>0)\,, \tag{B8}$$

where

$$U = \dot{\gamma}^2 \frac{S_{d-2}}{8(m+4)(2\pi)^{d-2}} \Gamma\left(\frac{d+m-2}{m+4}\right) \Gamma\left(\frac{14+2m-d}{m+4}\right) D_0 (\kappa\Lambda_0)^{\frac{2-d-m}{m+4}} \Lambda_x^{\frac{-14-2m+d}{m+4}} \lambda^{\frac{-16-m+2d}{m+4}}. \tag{B9}$$

$\Gamma(v)$ is the Gamma function and we have used

$$\int_0^\infty \frac{x^{z-1}dx}{(1+x)^{z+w}} = \frac{\Gamma(z)\Gamma(w)}{\Gamma(z+w)}, \qquad (\Re(z) > 0, \Re(w) > 0). \tag{B10}$$

The negative exponent of Λ_x in Eq. (B9) reveals the divergence established earlier and therefore reaffirms the necessity for coarse-graining.

Inserting the self energy (Eq. B8) into Eq. (3.19) leads to an expression for the recursion relation for Λ_x, which is most conveniently written in terms of the coupling constant U:

$$\frac{dU}{dl} = \frac{16+m-2d}{m+4} U - 2\frac{(14+2m-d)^2}{(m+4)(m+10-d)} U^2, \tag{B11}$$

where we have used Eq. (3.17) to eliminate z. Having thus removed the high wave vectors and rescaled all the parameters the final step of the RG analysis is to find the fixed points of Eq. (B11) for which the theory is invariant. Consistent with the previous determination of the critical dimension, the linear term changes sign for $d = d_c = (16+m)/2$. Since the quadratic term is negative for $d < m+10$ (or $d < d_c$ for $m < -4$), there is a non-zero stable fixed point

$$U^* = \frac{\epsilon}{9(d_c-6)} + \dots \tag{B12}$$

to first order in ϵ where $\epsilon = d - d_c$. This shows that the RG perturbation is well-behaved and the exponents are correct. For $d > d_c$ the only stable fixed point is $U^* = 0$, corresponding to an irrelevant non-linearity and recovering the exponents for the linear theory. Thus in the general case for $d + m - 2 > 0$,

$$\Lambda_x^* = \alpha_{m+1} \left[T^{4+m} \kappa^{2-d-m} \lambda^{-16-m+2d} \Lambda_0^{-2m-8} \dot{\gamma}^{2(4+m)} \right]^{1/(14+2m-d)}, \tag{B13}$$

$$\text{where} \qquad \alpha_{m+1} = \left[\frac{9S_{d-2}}{4(m+4)(2\pi)^{d-1}} \left(\frac{4+m}{16+m-2d}\right) \Gamma\left(\frac{d+m-2}{m+4}\right) \Gamma\left(\frac{14+2m-d}{4+m}\right) \right]^{(4+m)/(14+2m-d)}. \tag{B14}$$

We may apply this result to two of the relaxation mechanisms that we considered; both results are found in Table I in Section IV. For the permeable case, $d = 3$ and $m = 0$,

$$\Lambda_x^* = \alpha_1 \frac{T^{4/11} \Lambda_0^{3/11}}{\kappa^{1/11} \lambda^{10/11}} \dot{\gamma}^{8/11}, \qquad \text{where} \qquad \alpha_1 = \left[\frac{189 S_1}{2560\pi^2} \Gamma\left(\frac{1}{4}\right) \Gamma\left(\frac{3}{4}\right) \right]^{4/11} \simeq 0.342\ . \tag{B15}$$

For the confined case, $d = 3$ and $m = 2$,

$$\Lambda_x^* = \alpha_3 \frac{T^{2/5} \Lambda_0^{4/5}}{\kappa^{1/5} \lambda^{4/5}} \dot{\gamma}^{4/5}, \qquad \text{where} \qquad \alpha_3 = \left[\frac{45 S_1}{256\pi^2} \Gamma^2\left(\frac{1}{2}\right) \right]^{2/5} \simeq 0.378\ . \tag{B16}$$

A similar analysis cannot be conducted for the case $d = 3, m = -1$. In the hydrodynamic limit a divergence in the lower limit in the $k_\perp$ integral of Eq. (B7) occurs for $d + m - 2 \leq 0$. By introducing a lower cutoff given by the inverse collision length of the system L_p^{-1} and writing the integral in terms of the dimensionless quantity $y = L_p^3 \Lambda_x \lambda^2 / \kappa\Lambda_0$, the expression for the self energy for $d = 3, m = -1$ becomes

$$\Sigma(\boldsymbol{q}, 0) = -\frac{\alpha_0 \dot{\gamma}^2 D_0}{\lambda^3 \Lambda_x^3} \left[3\left(\ln(y+1) - \frac{y}{y+1} \right) - \frac{y^2}{(y+1)^2} \right] \Lambda_x q_x^2 l, \qquad \text{where} \qquad \alpha_0 = \frac{S_1}{96\pi^2} \simeq 0.000528. \tag{B17}$$

We now proceed as before by combining Eq. (3.19) and the expression for the self-energy (Eq. B17) to give the differential flow equation in terms of y,

$$\frac{dy}{dl} = y \left[-1 + \frac{\alpha_0 \dot{\gamma}^2 D_0}{\lambda^3} \left(\frac{L_p^3 \lambda^2}{\kappa \Lambda_0 y} \right)^3 \left[3\left(\ln(y+1) - \frac{y}{y+1} \right) - \frac{y^2}{(y+1)^2} \right] \right]. \tag{B18}$$

The unstable fixed point corresponding to the irrelevant non-linearity is given by $\Lambda_x = 0$. As we are unable to give an analytic expression for the stable fixed point solution of Eq. (B18) we show instead its power series in $\dot{\gamma}^2$,

$$\Lambda_x^* = \alpha_0 \frac{T L_p^6 \lambda}{\kappa^2 \Lambda_0} \dot{\gamma}^2 \left[1 - \frac{3}{2} \left(\alpha \frac{L_p^9 \lambda^3}{\kappa^3 \Lambda_0^2} \right)^2 \dot{\gamma}^4 + \mathcal{O}(\dot{\gamma}^5) \right]. \tag{B19}$$

Hence for small strain rates $\Lambda_x^* \sim \dot{\gamma}^2$.

3. First step coarse-graining

Here we demonstrate the procedure for a "first step" coarse-graining of the self-energy in Section III D, i.e. we calculate Λ_x by perturbing about the trivial fixed point $\Lambda_x^* = 0$. First we return to the expression for the coarse-grained self-energy in Eq. (B4) derived from Eq. (B1). Upon coarse-graining in the x direction, the limits of the sum and the integration are changed according to Eq. (B6). However, due to being far from the scaling regime, the assumption that $|\boldsymbol{k}| \to |\boldsymbol{k}_\perp|$ no longer holds. Hence in the limit $\Lambda_x \to 0$ (and thus $D_x \to 0$) appropriate for a "first step" coarse-grain, the integral becomes

$$\Sigma(\boldsymbol{q}, 0) = -\dot{\gamma}^2 q_x^2 \frac{D_0}{2(\kappa \Lambda_0)^2} \int_{\lambda e^{-l}}^{\lambda} \frac{dk_x}{2\pi} \int_0^\infty \frac{k^{d-3} dk S_{d-2}}{(2\pi)^{d-2}} \left[\frac{1}{4|\boldsymbol{k}|^{8+m}} + \frac{2k_x(k_x^3 + k_x k_\perp^2)}{2|\boldsymbol{k}|^{12+m}} \right] + \mathcal{O}(q_x^4) \tag{B20}$$

from which we may compute the self-energy for general m and d,

$$\Sigma(\boldsymbol{q}, 0) = -\beta \frac{T}{\kappa^2 \Lambda_0 \lambda^{9+m-d}} \dot{\gamma}^2 q_x^2 l. \tag{B21}$$

β is a numerical prefactor that depends on the relaxation mechanism m and the dimension d,

$$\begin{aligned} \beta = \frac{S_{d-2}}{8(2\pi)^{d-1}} \Gamma\left(\frac{d-2}{2}\right) \Gamma\left(\frac{10+m-d}{2}\right) \left[\Gamma\left(\frac{12+m}{2}\right) \right]^{-1} \\ \times \left[5 \left(\frac{12+m-d}{2}\right) \left(\frac{10+m-d}{2}\right) + 6 \left(\frac{d-2}{2}\right) \left(\frac{10+m-d}{2}\right) + \frac{d}{2} \left(\frac{d-2}{2}\right) \right]. \end{aligned} \tag{B22}$$

On substituting Eq. (B21) into the recursion relation for around the trivial fixed point (Eq. 3.21) we find that,

$$d\Lambda_x(l) \simeq \beta \frac{T}{\kappa^2 \Lambda_0 \lambda^{9+m-d}} \dot{\gamma}^2 l, \tag{B23}$$

which leads to the "tension" that depends on the cutoff in Eq. (3.22).

[1] W. Helfrich, Z. Naturforsch. **33a**, 305 (1978).
[2] O. Diat, D. Roux, and F. Nallet, J. Phys. II (France) **3**, 1427 (1993).
[3] P. Sierro and D. Roux, Phys. Rev. Lett. **78**, 1496 (1997).
[4] J. Yamamoto and H. Tanaka, Phys. Rev. Lett. **74**, 932 (1995).
[5] D. R. M. Williams and F. C. MacKintosh, Macromolecules **27**, 7677 (1994).
[6] G. K. Auernhammer, H. R. Brand, and H. Pleiner, Rheol. Acta **39**, 215 (2000).
[7] S. W. Marlow and P. D. Olmsted, (unpublished) (2002).
[8] A. G. Zilman and R. Granek, Eur. Phys. J. B **11**, 593 (1999).
[9] T. Hwa and M. Kardar, Phys. Rev. A **45**, 7002 (1992).
[10] A. J. Bray, A. Cavagna, and R. D. M. Travasso, Phys. Rev. **E 64**, 012102 (2001).
[11] A. J. Bray, A. Cavagna, and R. D. M. Travasso, Phys. Rev. **E 65**, 016104 (2001).
[12] L. Golubovic and T. C. Lubensky, Phys. Rev. B **39**, 12110 (1989).
[13] F. Brochard and J. F. Lennon, J. Phys. (France) **11**, 1035 (1975).
[14] R. Messager, P. Bassereau, and G. Porte, J. Phys. (France) **51**, 1329 (1990).
[15] M. Goulian and S. T. Milner, Phys. Rev. Lett. **74**, 1775 (1995).
[16] R. Bruinsma and Y. Rabin, Phys. Rev. **A45**, 994 (1992).
[17] S. Ramaswamy, Phys. Rev. Lett. **69**, 112 (1992).

[18] A. Al kahwaji and H. Kellay, Phys. Rev. Lett. **84**, 3073 (2000).
[19] M. E. Cates and S. T. Milner, Phys. Rev. Lett. **62**, 1856 (1989).
[20] G. H. Fredrickson, J. Chem. Phys. **85**, 5306 (1986).
[21] P. C. Hohenberg and B. I. Halperin, Rev. Mod. Phys. **49**, 435 (1977).
[22] S.-K. Ma, *Modern Theory of Critical Phenomena* (Benjamin Cummings, Reading, MA, 1976).
[23] A. Onuki and K. Kawasaki, Ann. Phys. **121**, 456 (1979).
[24] S. A. Wunenberger, Ph.D. thesis, Université Bordeaux (2001).
[25] S. Lerouge, G. Wilkins, S. W. Marlow, P. D. Olmsted, unpublished.
[26] S. Ramaswamy, J. Prost, W. Cai, and T. C. Lubensky, Europhys. Lett. **23**, 271 (1993).
[27] M. Criado-Sancho, D. Jou, and J. Casas-Vazquez, J. Phys. Chem. B **102**, 5335 (1998).
[28] C. Meyer, S. Asnacios, C. Bourgaux, and M. Kleman, Rheol. Acta **39**, 223 (2000).
[29] J. Zipfel, J. Berghausen, P. Lindner, and W. Richtering, J. Phys. Chem. B **103**, 2841 (1999).
[30] P. Boltenhagen, M. Kleman, and O. D. Lavrentovich, J. Phys. II (France) **4**, 1439 (1994).
[31] J. Leng, F. Nallet, and D. Roux, Eur. Phys. J. E **4**, 77 (2001).
[32] Since the range of wave vectors from d^{-1} to $L_p^{-1} \sim [d\sqrt{\kappa/T}]^{-1}$ is often very small or non-existent in a lamellar phase, general applicability of this theory is unclear.